

# Integrated Green's Function Molecular Dynamics Method for Multiscale Modeling of Nanostructures: Application to Au Nanoisland in Cu<sup>1</sup>

V.K. Tewary<sup>2</sup> and D.T. Read<sup>2</sup>

**Abstract:** An integrated Green's function and molecular dynamics technique is developed for multiscale modeling of a nanostructure in a semi-infinite crystal lattice. The equilibrium configuration of the atoms inside and around the nanostructure is calculated by using molecular dynamics that accounts for nonlinear interatomic forces. The molecular dynamics is coupled with the lattice statics Green's function for a large crystallite containing a million or more atoms. This gives a fully atomistic description of a nanostructure in a large crystallite that includes the effect of nonlinear forces. The lattice statics Green's function is then related to the anisotropic continuum Green's function that is used to model the free surface and also to relate the discrete lattice distortion to measurable parameters such as the displacement and the strain fields at the free surface. Thus the model seamlessly links the length scales from sub-nano in the core of the nanostructure to macroscopic parameters at the free surface. The model is applied to calculate the equilibrium configuration of atoms in and around an Au nanoisland embedded in fcc Cu, and the displacement and the strain fields on a free (0,0,1) surface in fcc Cu in which the nanoisland is embedded.

**keyword:** multiscale modeling, lattice statics Green's functions, molecular dynamics, strain field, nanoislands, Au in Cu

## 1 Introduction

Currently there is a strong scientific and technological interest in nanostructures such as quantum dots, metallic nanoislands, etc. embedded in a matrix. The semiconductor quantum dots have potential applications to extremely efficient solid state devices. Similarly, metallic

nanostructures are attracting a lot of attention because of their novel electronic and magnetic properties. The phenomenology and potential future uses of materials produced by the deposition of nanoclusters of metal atoms on surfaces were reviewed recently by Binns (2001). These materials have also attracted efforts to model their behavior by molecular dynamics, for example by Palacios (1999) and several others.

Modeling offers insight into, and possible prediction of, the behavior of the clusters, such as their preferred location and configuration as a function of size and energy of the incident particle and the temperature and structure of the substrate. It is, however, necessary to use multiscale modeling techniques for nanomaterials since conventional models based upon continuum mechanics are not fully applicable to nanostructures. Excellent reviews of the current perspective of computational nanotechnology and some specific techniques for multiscale modeling have been given by Srivastava and Atluri (2002), Ghoniem and Cho (2002), Shen and Atluri (2004), and Zhigilei and Dongare (2002).

Here we describe an integrated Green's function and molecular dynamics based multiscale modeling method for nanoislands of one material within a host lattice of a different material. The advantage of this method is that it can predict observable surface signatures above nanoislands buried within the host material. It also gives the strain field surrounding the nanoisland, which controls the interaction of the nanoisland with the surface and with other clusters. The strain field due to a nanoisland is an important characteristic of the material because it largely determines the self assembly of nanostructures, which is a promising method of fabricating large arrays of nanostructures.

Our method is generally applicable to nanostructures such as quantum dots or metallic nanoislands. In this paper we illustrate our technique by applying it to a gold (Au) nanoinclusion in copper (Cu). We calculate the

<sup>1</sup>Contribution of the National Institute of Standards and Technology, an agency of the US Govt. Not subject to copyright in the USA.

<sup>2</sup>N.I.S.T., Boulder, CO, USA

elastic characteristics of an Au nanoinclusion in fcc Cu lattice by using a multiscale model that links seamlessly the subnano meter (atomistic) scale to the micrometer scale and to macro continuum scales in solids. We model the full discrete fcc lattice structure of the Au nanoinclusion, and the embedding host Cu lattice consisting of a million atoms. In addition, our model accounts for a free surface in the host lattice. We calculate the discrete lattice distortion in and around the nanoinclusion and the resulting continuum strain and the displacement fields due to the nanoinclusion on the free surface of the Cu lattice. The seamless relationship between the discrete lattice distortions that are defined as discrete variables at the subnanometer scale and the strain and the displacement fields that are continuum variables at the macro scale is achieved by our new multiscale modeling technique. The strain and the displacement fields can be measured at the free surface and can be used to characterize the elastic properties of the composite Au/Cu materials system.

The presence of a nanoinclusion in an otherwise perfect host lattice can be treated as a lattice defect. The defect causes distortion of the host lattice. At the atomistic level the lattice distortion is expressed in terms of the displacements of atoms from their original lattice sites which are difficult to measure. In the continuum model of the solid, the lattice distortion is expressed as the strain or the displacement field. These are very important parameters that characterize the elastic properties of the defect.

In order to interpret the experimental results on strain and the displacement fields, one needs to calculate these quantities at a free surface since that is where the measurements are usually made. The free surface itself is a defect in the lattice, which is normally modeled as an infinite solid. Hence the free surface changes the lattice distortion caused by the defect. It is therefore necessary to model a lattice containing a nanoinclusion as well as a free surface. Presently, multiscale models are not available in the literature that treat the nanostructure in a fully discrete manner and account for free surface in the host lattice.

A purely discrete lattice model of a free surface would require very extensive computational effort and still suffer from some fundamental uncertainties such as that in the interatomic potential. Good model interatomic potentials are available for atoms in the bulk of the crystal but they may not be valid at the surface because of the rearrangements of electronic orbitals. On the other

hand, an extended macroscopic defect like a free surface can be adequately modeled by using the continuum theory by imposing the free surface boundary condition on the Christoffel equation. During the past several decades, the continuum model [Ting(1996)] has been extensively and successfully used for modeling the elastic response of solids containing extended defects such as a free surface. Our approach, therefore, is to develop a multiscale model that uses discrete atomistic theory to model the lattice in and around the nanoinclusion and use the continuum theory to model the free surface in a unified integrated formalism.

A mathematical model representing a lattice containing a nanoinclusion and a surface needs to satisfy the following criteria: (i) the theory must account for the discrete lattice structure of the lattice in and around the nanoinclusion and, therefore the model crystallite must be sufficiently larger than the nanoinclusion, (ii) the model crystallite must be large enough to include a free surface and for the lattice distortions to smear out into a continuum so that the continuum parameters like the strain and the displacement fields can be defined, (iii) the continuum parameters have to account for the elastic anisotropy since most materials of practical interest are anisotropic, (iii) the theory must include nonlinear interactions between atoms inside and close to the nanoinclusion even if the host lattice is harmonic, and, finally (iv) the model should be computationally efficient so that the calculations can be carried out on an ordinary desktop which would enable a researcher to get quick answers to 'what if' type questions in the design of experiments.

The criteria (i), (ii), and (iii) require the model to be multiscale and bridge the length scales from the atomistic through to the macro continuum. None of the existing models in the literature (for review and other references, see, for example, [Ortiz and Phillips (1999), Phillips (1998)]) meet all the above four criteria. The lattice statics Green's function (LSGF) method [Tewary (1973), Thomson et. al (1992)] is computationally efficient and can model large crystallites but does not account for the nonlinear interactions. The molecular dynamics (MD) accounts for nonlinear forces but is usually limited to crystallites of only a few hundred atoms. Powerful techniques based upon MD have been developed by Vashishta, Kalia, and Nakano (2003) to model crystallites containing up to 10 million atoms but these techniques are computationally intensive. MD calcula-

tions using flexible boundary conditions derived from the Green's function [see, for example, Rao et. al. (1998), Sinclair et. al. (1978)] and purely numerical techniques [see, for example, Tadmore et. al. (1996)] based upon finite element methods have been developed for some defect systems. No existing multiscale modeling technique has been applied to a nanoinclusion and a free surface in a large model crystallite, which is the object of our paper. Earlier, we [Tewary (2004)] presented a multiscale Green's function (MSGF) technique to model a point defect and a free surface in a fcc solid. This technique integrates the LSGF with the continuum Green's function (CGF) and is specifically meant for point defects in a large crystallite containing a free surface. A similar technique has also been applied [Tewary and Yang (2003)] to a Ge quantum dot in Si but without including nonlinear effects which are expected to be significant in the core of a nanostructure. In this paper, we extend this technique substantially to account for the nonlinear forces in the core using MD and apply it to a nanoinclusion in a million-atom model crystallite containing a free surface. Our model integrates MD, LSGF, and CGF and meets all the 5 criteria given above. We will refer to our model as the GFMD model.

We use the Born van Karman model as the reference state for the host lattice. In this model, the crystal Hamiltonian is given by the interatomic force constants and the forces on each lattice site in a lattice without defects are zero. The presence of a defect in a lattice exerts direct forces on the atoms and changes the interatomic force constants within the range of interatomic interactions from the defect and also changes the response or the Green's function of the whole lattice. The lattice Green's function of the solid with defects is called the defect GF and is related to the perfect GF through the Dyson equation. In the LSGF method one divides the vector space of the whole lattice in a localized defect space where the forces and the change in the crystal Hamiltonian are non zero and a perturbed host lattice space where these changes are zero. The displacements in the entire solid are given by the product of the defect GF and the direct forces due to the defect.

Instead of using the defect GF, it is possible to write the displacements in an alternative form [Tewary (1973)] as a product of the perfect LSGF and effective Kanzaki forces. The Kanzaki forces are nonzero only in the defect space. The advantage of writing the solution in this

form is that the perfect LSGF reduces asymptotically to the CGF which can then be used to model an extended defect like a free surface using the powerful techniques of the continuum theory. The Kanzaki forces contain the full contribution of the discrete structure of the lattice in the defect space and are obtained by solving the Dyson equation in the defect space. We use this correspondence between the perfect LSGF and the CGF to incorporate the effect of the free surfaces in our GFMD model. In contrast, the defect GF does not [Tewary (2002,2004)] reduce to the CGF except in the limit when the contribution of the defect itself becomes negligible. A technique based upon replacing the defect GF by the CGF, therefore, will not give a reliable representation of the interaction between nanostructures and free surfaces.

Since the host lattice is assumed to be harmonic, the nonlinear effects, if any, are localized close to the defect. We include the entire region where nonlinear effects are significant in the defect space. We model the defect space by using MD and calculate the Kanzaki forces on all atoms in the defect space. The Kanzaki forces are then used to calculate the displacements in the entire lattice outside the defect space. The defect space, which we treat by using MD, consists of 17169 atoms. The host lattice which consists of a million atoms is treated in our model by using the LSGF method. In the asymptotic limit, far from the defect space we use the continuum Mindlin Green's function to include the effect of the free surface and also to calculate the elastic strain and the displacement field at the surface. Powerful techniques [see, for example, Pan (2002), Pan and Yuan (2000), Pan and Yang (2001)] for calculating the Mindlin Green's function are available in the literature.

In our calculations, we use the many-body interatomic potential derived by Cleri and Rosato (1993) between Au-Au, Au-Cu, and Cu-Cu atoms. This potential extends up to 5th neighbor distance and correctly reproduces many observable physical properties of the bulk solid such as vacancy formation energy, phonon frequencies, elastic constants, etc. Recently this potential has been used by Sandberg and Grimvall (2001) to calculate the anharmonic contribution to the formation enthalpy of a vacancy in Cu at high temperatures.

The theory of our GFMD model is described in Sec. II. The application of the GFMD model to an Au nanoisland in Cu is given in Sec. III which gives the calculated values of the nonlinear lattice distortion in and around

the nanoinclusion and the elastic strain and displacement fields at the free (1,0,0) surface. Finally a brief discussion of the results and conclusions are presented in Sec. IV.

## 2 Theory and application of the GFMD model to Au nanoinclusion in Cu

We consider the Born von Karman model [Maradudin et. al. (1971)] of a monatomic fcc Bravais lattice assuming short-range interatomic interactions. The treatment given here, therefore, is not as such applicable to ionic solids that have long-range Coulomb interactions. We assume a Cartesian frame of reference with an atomic site as origin and the coordinate axes parallel to the crystallographic axes. We denote the lattice sites by vector indices  $\mathbf{l}$ ,  $\mathbf{l}'$  etc. A vector index  $\mathbf{l}$  has 3 components denoted by  $l_1$ ,  $l_2$ , and  $l_3$ . The Cartesian indices will be denoted  $i$ ,  $j$ ,  $k$ , etc. Summation over repeated Cartesian indices is assumed.

The 3 x 3 force constant matrix between atoms at  $\mathbf{l}$  and  $\mathbf{l}'$  will be denoted by  $\mathbf{l}, \mathbf{l}'$ . The  $(i,j)$  matrix element  $\phi_{ij}(\mathbf{l}, \mathbf{l}')$  of the force constant matrix gives the force on the atom  $\mathbf{l}$  in the direction  $i$  if the atom  $\mathbf{l}'$  is displaced by a unit amount in the direction  $j$ . The force on atom  $\mathbf{l}$  and its displacement from equilibrium position will be denoted, respectively, by  $\mathbf{F}_t(\mathbf{l})$  and  $\mathbf{u}(\mathbf{l})$ , which are 3d (3-dimensional) vectors or 3x1 column matrices. The displacement vectors  $\mathbf{u}(\mathbf{l})$  at each lattice site give the relaxation of the lattice or the lattice distortion caused by the defect. In the representation of the lattice sites,  $\phi$  can be regarded as a 3N x 3N matrix where N is the number of atoms in the Born von Karman supercell. In the same representation,  $\mathbf{F}$  and  $\mathbf{u}$  are 3N x 1 column matrices.

The potential energy of the crystal can be written as follows:

$$W^* = \sum_{\mathbf{l}} W_{\mathbf{l}}(x_{\mathbf{l}}), \quad (1)$$

where

$$x_{\mathbf{l}} = \mathbf{r}_{\mathbf{l}} + \mathbf{u}_{\mathbf{l}} \quad (2)$$

denotes the instantaneous position of the atom  $\mathbf{l}$ ,  $\mathbf{r}_{\mathbf{l}}$  its equilibrium lattice site, and  $W_{\mathbf{l}}$  is its potential energy in the field of all other atoms. The sum over  $\mathbf{l}$  in Eq. (1) extends over all the atoms in the crystal. A perfect lattice with no defects has translation symmetry, so the form of the potential energy function is same for all the

atoms so the function  $W_{\mathbf{l}}$  is independent of  $\mathbf{l}$ . We also assume that the perfect lattice is purely harmonic, that is, the interaction between the host atoms when they are located at or near the perfect lattice sites, can be represented by a series containing up to quadratic power of displacements. In the Born von Karman approximation the emphasis is on the second and higher derivatives of the energy. The reference value is set to zero arbitrarily, and the first derivative is zero by definition of the equilibrium lattice spacing.

We assume a model in which  $n_A$  sites of the host lattice at the center of the supercell are occupied by foreign atoms. All the foreign atoms are assumed to be of the same kind, which fill all the fcc lattice sites in a cube of edge length  $2A$  centered at the origin of the coordinates. We shall refer to this cube as the inner core of the defect in contrast to the outer core and the shell to be defined later.

We further identify a cube of edge length  $2B$  that encloses the  $n_A$  foreign atoms and  $n_B$  host atoms such that the total number of lattice sites in the outer cube are  $n_A + n_B$ . This outer cube is also centered at the origin of coordinates. We will refer to the region between the outer cube of edge length  $2B$  and the inner cube of edge length  $2A$  as the outer core. We will refer to the combined inner and outer core as the core cube or the defect cube. The size of the outer cube is chosen such that it includes at least all those atoms with which the atoms of the inner core interact directly. It may include some extra atoms in order to form a complete cube with all lattice sites occupied. Obviously, in this model the atoms of the inner core will not directly interact with any atom of the host lattice outside the outer cube.

The core cube of edge length  $2B$  is treated as the defect in our model lattice. All lattice sites in the supercell outside the core are occupied by the atoms of the same kind as the host. We further identify a shell region by drawing another cube of edge length  $2C$  containing  $n$  lattice sites that encloses the defect cube and is also centered at the origin of the coordinates. The size of the shell cube is assumed to be much smaller than the size of the Born von Karman supercell. We will refer to this outermost cube as the shell cube and the region between the shell cube and the core cube as the shell region. If  $n_C$  is the number of lattice sites in the shell region then  $n = n_C + n_B + n_A$ . All  $n_C$  lattice sites of the shell region are occupied by the atoms of the same kind as the host. The region of the supercell outside the shell cube will be referred to as the

host region.

Now we write the total potential energy of the entire crystal given by Eq. (1) in the following form:

$$W^* = \sum_{\mathbf{I}^*} W_h(x_{\mathbf{I}^*}) + \sum_{\mathbf{I}^s} W_{h'}(x_{\mathbf{I}^s}) + \sum_{\mathbf{L}} W_c(x_{\mathbf{L}}), \quad (3)$$

where  $W_h$  is the potential function for a host atom which is interacting only with other host atoms,  $W_{h'}$  is the potential function for a host atom interacting with other host atoms as well as atoms in the defect cube, and  $W_c$  is the potential function of an atom in the defect cube interacting with other defect or host atoms. The superscripts \*, s, and c over the summation signs on the right hand side (RHS) of Eq. (3) indicate that the summation is over a limited range of sites: the index  $\mathbf{I}^*$  goes over all lattice sites outside the shell cube. The index  $\mathbf{I}^s$  goes over all lattice sites in the shell region (excludes the core, both inner and outer), and  $\mathbf{L}$  goes over all the lattice sites of the defect (outer as well as inner core) cube. In the present paper we shall assume a many-body potential so each potential function would depend upon the coordinates of many atoms which will be specified later.

In this scheme of partition of the lattice into different regions as defined above, the terms in the first summation on the RHS of Eq. (3) depend explicitly upon the coordinates of the host atoms outside the shell cube and inside the shell region. The terms in the second summation on the RHS depend explicitly upon the coordinates of the host atoms outside the shell cube, inside the shell region, and in the outer core of the defect cube. They do not depend upon the coordinates of the foreign atoms that are confined to the inner core. The foreign atoms do not interact directly with the host atoms in the shell region and beyond. The terms in the third summation on the RHS depend explicitly upon the coordinates of the foreign and the host atoms in the core and the shell regions.

We rewrite Eq. (3) as follows:

$$W^* = W_0 + \Delta W, \quad (4)$$

where

$$W_0 = \sum_{\mathbf{I}} W_h(x_{\mathbf{I}}), \quad (5)$$

$$\Delta W = \sum_{\mathbf{I}^s} \Delta W_{h'}(x_{\mathbf{I}^s}) + \sum_{\mathbf{L}} \Delta W_c(x_{\mathbf{L}}) \quad (6)$$

$$\Delta W_{h'}(x_{\mathbf{I}^s}) = W_{h'}(x_{\mathbf{I}^s}) - W_h(x_{\mathbf{I}^s}), \quad (7)$$

and

$$\Delta W_c(x_{\mathbf{L}}) = W_c(x_{\mathbf{L}}) - W_h(x_{\mathbf{L}}). \quad (8)$$

The sum in Eq. (5) is over all the lattice sites of the perfect lattice and  $W_0$  gives the energy of the perfect but distorted lattice when the crystal does not contain any foreign atoms and the atoms are located at  $\mathbf{x}_{\mathbf{I}}$  given by Eq. (2). We define this distorted perfect lattice as our reference state. The interaction between each atom in the perfect lattice is assumed to be harmonic. The harmonic energy in the reference state will be given later in Eq. (9). The change in the energy of the reference state caused by the presence of the defect is given by  $\Delta W$ .

We further assume that the atomic displacements in the shell region are so small that their cubic and higher powers can be neglected in the Taylor expansion of the potential energy. If the displacements in the shell regions were large, then we would choose a larger inner core such that these displacements are small enough for the harmonic approximation to be valid. Hence the interaction between the shell atoms amongst themselves and with the atoms in the host region can be assumed to be harmonic. On the other hand the displacements of the atoms in the core cube may be large. Hence the interaction between the atoms in the shell region and those in the outer core may be nonlinear. In general, the interaction between the atoms in the core will be nonlinear.

Now we write the potential energy of each atom in the reference state. The potential energy of each atom is a sum of its interaction potential with all its neighboring atoms and depends upon the coordinates of all the atoms contributing to the interaction potential. In the harmonic approximation, the potential energy of the reference lattice is given by [Tewary (1973), Maradudin et al. (1971)] the following Taylor series:

$$W_0 = \sum_{\mathbf{I}} F_{0i}(\mathbf{I}) u_i(\mathbf{I}) + (1/2) \sum_{\mathbf{I}'} [\phi(\mathbf{I}, \mathbf{I}')]_{ij} u_i(\mathbf{I}) u_j(\mathbf{I}'), \quad (9)$$

where

$$F_{0i}(\mathbf{I}) = - \sum_{\mathbf{I}'} [\partial W_h(x_{\mathbf{I}^s}) / \partial u_{i\mathbf{I}}]_{\mathbf{0}}, \quad (10)$$

$$[\phi(\mathbf{I}, \mathbf{I}')]_{ij} = \sum_{\mathbf{I}''} [\partial^2 W_h(x_{\mathbf{I}^s}) / \partial u_{i\mathbf{I}} \partial u_{j\mathbf{I}''}]_{\mathbf{0}}, \quad (11)$$

and  $\mathbf{I}''$  in Eq. (9) goes over all the lattice sites of the reference lattice. The derivatives in Eqs. (10) and (11) are evaluated at 0 displacements. In what follows, for brevity, we will not explicitly show the Cartesian indices

$i, j$ , etc except when needed to avoid any confusion. It will be understood that the derivatives are defined with respect to individual Cartesian components of the displacements as in Eqs. (10) and (11).

In our model, we shall assume a many-body potential function derived by Cleri and Rosato (1993) for the interatomic interactions. This potential extends up to 5th neighbors of each atom and depends upon the coordinates of 79 atoms in fcc structure. The summations in Eqs. (10) and (11) extend over all the atoms in the reference lattice whose potential energy depends upon the displacement of the reference atom  $\mathbf{l}$ . For the same reason, although  $\phi(\mathbf{l}, \mathbf{l}')$  relates only a pair of atoms, in case of a many-body potential as considered in this paper, it depends upon the coordinates all the atoms included in the many-body potential. In case of the reference lattice, the linear term  $\mathbf{F}_0(\mathbf{l})$  in the Taylor series in Eq. (9) is 0 for all  $\mathbf{l}$  because of the translation symmetry and the equilibrium condition [Maradudin et. al. (1971)]. The higher order terms in Eq. (9) are neglected in the harmonic approximation.

The atomic displacements at equilibrium are obtained by minimizing the total energy of the defect state given by Eq. (4) which gives

$$\partial W_0(\mathbf{x}_\mathbf{l})/\partial \mathbf{u}_\mathbf{l} = \mathbf{F}_t(\mathbf{l}), \quad (12)$$

where

$$\mathbf{F}_t(\mathbf{l}) = -\partial[\sum_{\mathbf{l}'}^s \Delta W_h(\mathbf{x}_{\mathbf{l}'}) + \sum_{\mathbf{l}}^c \Delta W_c(\mathbf{x}_{\mathbf{l}})]/\partial \mathbf{u}_\mathbf{l}. \quad (13)$$

Using Eq. (11), we write Eq. (12) in the matrix notation as follows

$$\phi \mathbf{u} = \mathbf{F}_t. \quad (14)$$

The solution of Eq. (14) is

$$\mathbf{u} = \mathbf{G}\mathbf{F}_t, \quad (15)$$

where  $\mathbf{G}$ , the Green's function matrix [Tewary (1973), Maradudin et. al. (1971)], is the inverse of  $\phi$ . So

$$\mathbf{G}(\mathbf{l}, \mathbf{l}')\phi(\mathbf{l}, \mathbf{l}') = \delta(\mathbf{l}, \mathbf{l}'), \quad (16)$$

where  $\delta(\mathbf{l}, \mathbf{l}')$  is the Dirac's delta function which is 1 for  $\mathbf{l} = \mathbf{l}'$  and 0 otherwise.

From Eq. (15), the atomic displacement of the atom  $\mathbf{l}$  can be written explicitly as

$$\mathbf{u}_\mathbf{l} = \sum_{\mathbf{l}'} \mathbf{G}(\mathbf{l}, \mathbf{l}')\mathbf{F}_t(\mathbf{l}'). \quad (17)$$

The summation in Eq. (17) is over all the lattice sites occupied by the host as well as the foreign atoms. First, we note that  $\mathbf{F}_t(\mathbf{l})$  is 0 for all  $\mathbf{l}$  in the host region because of the following. The contribution of the first term in Eq. (13) to the force on the atoms of the host region is 0 since the two terms in Eq. (7) will cancel out. The contribution of the second term in Eq. (13) is also 0 because the atoms in the core region do not interact directly with the atoms in the host region and hence do not exert any force on the atoms in the host region. We can therefore restrict the summation in Eq. (17) to the shell and the core regions.

The vector space of all sites in the shell and the core regions can now be identified as the defect space as defined in [Tewary (1973)]. Equation (17) gives the lattice distortion in terms of the perfect LSGF instead of the defect GF, and a force term that is calculated at the relaxed lattice sites instead of the original lattice sites. We can, therefore, identify  $\mathbf{F}_t$  as the Kanzaki force defined in Tewary (1973). The solution given by Eq. (17) is equivalent to that obtained in terms of the defect GF which is given by the solution of the Dyson's equation [Tewary (1973), Maradudin et. al. (1971)] in the defect space. The defect GF technique [Tewary (1973)] is applicable to weak defects when the harmonic approximation is valid for  $\Delta W$ .

Equation (17) is a formal solution of the problem but its RHS depend upon the displacements in the defect space which are yet to be determined. Our main objective is to calculate the atomic displacements outside the defect space which give the measurable strain and displacement fields but we need to calculate the displacements in the shell and the core region as well. First we consider the case when the index  $\mathbf{l}$  in Eq. (17) is restricted to atoms in the shell region outside the core cube. The index  $\mathbf{l}'$  in Eq. (17) is restricted to all the atoms in the defect space. Using Eqs. (7), (8), and (9), we write the following for the total force on an atom  $\mathbf{l}'$  inside the defect space

$$\mathbf{F}_t(\mathbf{l}') = \mathbf{F}_s(\mathbf{l}') + \mathbf{F}_c(\mathbf{l}') \quad (18)$$

where

$$\mathbf{F}_s(\mathbf{l}') = \partial[\sum_{\mathbf{l}''}^s W_h(\mathbf{x}_{\mathbf{l}''})]/\partial \mathbf{u}_{\mathbf{l}'} - \sum_{\mathbf{l}''}^{h,s,c} [\phi(\mathbf{l}', \mathbf{l}'')] \mathbf{u}(\mathbf{l}''), \quad (19)$$

$$\mathbf{F}_c(\mathbf{l}') = \partial[\sum_{\mathbf{l}}^c W_c(\mathbf{x}_{\mathbf{l}})]/\partial \mathbf{u}_{\mathbf{l}'} - \sum_{\mathbf{l}''}^{s,c} [\phi(\mathbf{l}', \mathbf{l}'')] \mathbf{u}(\mathbf{l}''). \quad (20)$$

The summation in the first term on the RHS of Eq. (19) is over the atoms in shell region which interact with the atom  $\mathbf{l}'$  that can be in the shell or the core. Similarly the sum over  $\mathbf{L}$  in Eq. (20) is over atoms in the core region which interact with the atom  $\mathbf{l}'$ . The summation in the second term on the RHS of Eq. (19) is over all atoms in the host, shell and core regions even though  $\mathbf{l}'$  is confined to the shell region. This is because of the range of interaction potential of the atom  $\mathbf{l}'$ . The same applies to Eq. (20) except that the range of interaction of an atom in the core does not extend to the host region.

We calculate the force on atom  $\mathbf{l}'$  in the shell region as given by Eq. (18). We consider the first term on the RHS of Eq. (19). An atom in the shell region interacts with atoms in the host region, the shell region, and the outer core. Thus

$$W_{h'}(\mathbf{x}_{l'}) = \sum^h W_h^h(\mathbf{x}_{l'}) + \sum^s W_h^s(\mathbf{x}_{l'}) + \sum^c W_h^c(\mathbf{x}_{l'}), \quad (21)$$

where the superscripts h, s, and c over W on the RHS of Eq. (21) denote contributions of the atoms from the host, shell, and core regions respectively to the potential energy of the atom  $\mathbf{l}'$  which is in the shell region. The first two terms on the RHS of Eq. (21) are the same as for host-host interactions. This explains why the subscript under W in these two terms is h and not h'. Since we have assumed the host-host interaction to be harmonic, we can expand the first two terms in a Taylor series. Thus, we obtain the following result for the contribution to the force from the first term in Eq. (19):

$$\mathbf{F}_{s1}(\mathbf{l}') = \sum_{h,s} \mathbf{F}^{h,s}(\mathbf{l}') + \mathbf{F}^{*c}(\mathbf{l}') + \sum_{h,s}^c \mathbf{l}' [\phi(\mathbf{l}', \mathbf{l}')] \mathbf{u}(\mathbf{l}'), \quad (22)$$

where  $\mathbf{F}^{h,s}(\mathbf{l}')$  denote the contribution to the force at the atom  $\mathbf{l}'$  from the host and the shell regions, and

$$\mathbf{F}^{*c}(\mathbf{l}') = -\partial W^c(\mathbf{l}') / \partial \mathbf{u}_l, \quad (23)$$

is the contribution to the potential energy of the atom  $\mathbf{l}'$  from the core atoms. The summation in the first term on the RHS of Eq. (22) is over all atoms in the host and the shell region which contribute to the force on  $\mathbf{l}'$ . Note that  $\mathbf{F}^{h,s}$  and  $\phi$  are the first and the second Taylor coefficients in the expansion of the potential energy and are evaluated at 0 displacements as given in Eqs. (10) and

(11). In contrast, the derivative in Eq. (23) is evaluated at the displaced position of the atom which includes the effect of all higher order terms.

We see from Eqs. (19) and (22) that the contributions of the host and the shell atoms to the term linear in displacement cancel out. Hence we obtain

$$\mathbf{F}_s(\mathbf{l}') = \mathbf{F}^{h,s}(\mathbf{l}') + \mathbf{F}^{*c}(\mathbf{l}') - \sum_{\mathbf{l}''}^c [\phi(\mathbf{l}', \mathbf{l}'')] \mathbf{u}(\mathbf{l}''). \quad (24)$$

Now we consider the contribution of a particular atom  $\mathbf{l}'' = \mathbf{L}'$  to the summation in the second term of Eqs. (24) where  $\mathbf{L}'$  is in the core cube. The contribution of this term to the displacement given by Eq. (17) is as follows:

$$\mathbf{u}_l = - \sum_{\mathbf{l}'}^s \mathbf{G}(\mathbf{l}, \mathbf{l}') \phi(\mathbf{l}', \mathbf{L}') \mathbf{u}(\mathbf{L}'), \quad (25)$$

where  $\mathbf{l}$  is outside the defect cube. Since  $\mathbf{L}'$  is in the core, all the atoms that interact with this atom are inside the shell or the core cubes and are therefore included in the summation in Eq. (25). In view of Eq. (16) the RHS of Eq. (25) is 0 since  $\mathbf{l} \neq \mathbf{L}'$ . Hence, for  $\mathbf{l}$  outside the core cube, the last term on the RHS of Eq.(20) does not contribute to the atomic displacements and can be neglected.

Finally, we recall that the total force at any atom in the reference state is 0. Hence

$$\sum_{h,s,c} \mathbf{F}^{h,s,c}(\mathbf{l}') = \mathbf{0} \quad (26)$$

for all  $\mathbf{l}'$ . This gives

$$\sum_{h,s} \mathbf{F}^{h,s}(\mathbf{l}') = -\mathbf{F}^c(\mathbf{l}'). \quad (27)$$

Using Eq. (27), Eq. (24) gives the following for  $\mathbf{l}'$  in the shell cube:

$$\mathbf{F}_s(\mathbf{l}') = -\mathbf{F}^c(\mathbf{l}') + \mathbf{F}^{*c}(\mathbf{l}'). \quad (28)$$

Proceeding as above we calculate  $\mathbf{F}_c(\mathbf{l}')$  given by Eq. (20) for  $\mathbf{l}'$  in the shell region. This force arises because the potential energy of the core atoms depends upon the coordinates of the shell atoms. For  $\mathbf{l}'$  in the shell region only the core atoms would contribute to the sum in the harmonic term on the RHS of Eq. (20). However, as we have shown earlier, the harmonic term arising from the displacement of the core atoms does not contribute to the displacements of the atoms in the shell and the host regions. Hence  $\mathbf{F}_c(\mathbf{l}')$  is given by only the first term in Eq.

(20). Finally, we obtain the following for the total force on an atom  $\mathbf{l}'$  in the shell region:

$$\mathbf{F}_t(\mathbf{l}') = -\mathbf{F}^c(\mathbf{l}') + \mathbf{F}^{*cc}(\mathbf{l}'), \quad (29)$$

where

$$\mathbf{F}^{*cc}(\mathbf{l}') = \mathbf{F}^{*c}(\mathbf{l}') - \partial \left[ \sum^c \mathbf{L} W_c(\mathbf{x}_L) \right] / \partial \mathbf{u}_{\mathbf{l}'}, \quad (30)$$

The last term on the RHS of Eq. (29) gives the total force exerted on a shell atom from the core atoms. The first term on the RHS of Eq. (30) arises from the potential energy of the shell atoms which depends upon the coordinates of the core atoms. The second term on the RHS of Eq. (30) arises from the potential energy of the core atoms which depends upon the coordinates of the shell atoms. Physically, Eq. (29) means that the effective force on an atom in the shell region is equal to the force exerted on the atom due the core atoms minus the force the core atom would have exerted if it were at the reference lattice site. This force arises from the potential energy of the shell atoms.

In order to use Eq. (17), we also need to calculate  $\mathbf{F}_t(\mathbf{l}')$  for  $\mathbf{l}'$  in the core cube. In this case, we obtain

$$\mathbf{F}_t(\mathbf{l}') = \mathbf{F}^{*sc}(\mathbf{l}') - \sum_{\mathbf{l}''} S_{\mathbf{l}'\mathbf{l}''} [\phi(\mathbf{l}', \mathbf{l}'')] \mathbf{u}(\mathbf{l}''), \quad (31)$$

where

$$\mathbf{F}^{*sc}(\mathbf{l}') = -\partial \left[ \sum_{\mathbf{l}''} S_{\mathbf{l}'\mathbf{l}''} W_h(\mathbf{x}_{\mathbf{l}''}) \right] / \partial \mathbf{u}_{\mathbf{l}'}, \\ - \partial \left[ \sum^c \mathbf{L} W_c(\mathbf{x}_L) \right] / \partial \mathbf{u}_{\mathbf{l}'}. \quad (32)$$

The force given by Eq. (32) is the total force on a core atom at its displaced position arising from the nonlinear interaction between the shell and the core atoms. The second term on the RHS of Eq. (31) gives the correction term arising from the use of the perfect lattice Green's function instead of the defect lattice Green's function. As described before, the displacements of atoms in the inner core do not contribute to the harmonic part of the force. The force arising out of the nonlinear interaction is relaxed to 0 in MD. Hence, the atoms of the inner core do not contribute directly to the summation in Eq. (17).

We need to first solve Eq (17) for the shell displacements with  $\mathbf{F}_t(\mathbf{l}')$  for the shell and the core atoms by Eqs. (29) and (31) respectively. We solve this set of nonlinear equations by first using MD in the defect space. For this purpose we consider the aggregate of all  $n$  atoms in

the defect space that includes the core cube and the shell cube. We fix the position of the atoms in the shell region to which the atoms in the defect space are coupled. We apply standard molecular dynamics to this aggregate with the boundary conditions that the  $n_C$  shell atoms are fixed at a position determined self consistently by Eq. (17). In actual practice, we obtain the solution by iteration as described below.

First we fix the  $n_C$  shell region atoms at their original lattice sites corresponding to  $\mathbf{u}(\mathbf{l})=0$  for the shell atoms. Then we use MD for the  $n_A + n_B$  atoms in the core. This gives equilibrium values of atomic displacements in the core and  $\mathbf{F}^{*sc} = 0$  for all atoms in the core cube but non-zero value of  $\mathbf{F}^{*cc}$ , that is the forces on the shell atoms due to the core. We use these forces in Eq. (17) to calculate the displacement of the shell atoms. These same forces also control the displacements of all the atoms in the host region. In the next iteration, we fix the  $n_C$  shell atoms at the new positions calculated from Eq. (17) in the previous step and repeat the MD for the core which, at equilibrium, gives additional forces on the shell atoms. We repeat the process until the solution converges. In the cases where we have applied this method, the solution converges to within 99% in a single iteration.

Once we get the forces  $\mathbf{F}_t(\mathbf{l}')$ , we can calculate the atomic displacements everywhere in the crystal by using the LSGF in Eq. (17). The calculation and properties of the lattice statics Green's function have been discussed in detail in [Tewary (1973), Thomson et. al. (1992)]. The calculation of the forces on atoms in the shell and the outer core, as described above, are done using a purely discrete atomistic model at the subnano scale. These forces contain the full information about the atomistic nature of the defect. The LSGF fully accounts for the discrete atomistic structure of the lattice over the scale of several atomic distances. For example, for a million atom model, the edge length of the supercell is of the order of 100 lattice constants.

One advantage of Eq. (17) is that it depends upon the perfect LSGF which can be conveniently expressed [Tewary (1973), Maradudin et. al. (1971)] in terms of its Fourier transform in the reciprocal space of the lattice. This could not be done for the defect GF [Tewary (1973), Maradudin et. al. (1971)]. The Fourier transform of the perfect LSGF can be calculated by using the dynamical matrix of the lattice defined in terms of the force constants [Tewary (1973), Maradudin et. al. (1971)].

Since the forces and the displacements are specified at discrete lattice sites, they can also be expressed [Tewary (1973)] in terms of their Fourier transforms in the same space. This provides a computationally convenient technique for calculating the LSGF and the atomic displacements.

Another advantage of using the perfect lattice GF in Eq. (17) is that it can link the atomistic calculations seamlessly to the continuum model as has been done for a vacancy in Cu [Tewary (2004)]. The atomic displacements obtained from Eq. (17) using the lattice statics GF are defined at discrete lattice points. In many applications, one needs elastic strains which are also measured experimentally. Strain is a continuum parameter defined in terms of the derivatives of the displacement field and can not be defined as such for discrete values of the displacements. In our model, we achieve the correspondence between the discrete atomistic displacements and the continuum displacement field by using the property [Tewary (1973), Tewary (2004)] that the LSGF reduces to the CGF asymptotically at large distances. We simply use the CGF for the  $\mathbf{G}(\mathbf{l}, \mathbf{l}')$  in Eq. (17) treating  $(\mathbf{r}_1 - \mathbf{r}_1')$  as a continuous variable while treating  $\mathbf{l}'$  as a discrete variable corresponding to atoms in the shell and the core cubes where the discrete forces are calculated. The strains are then calculated by taking appropriate derivatives with respect to  $\mathbf{r}_1$ . Efficient techniques for calculating the continuum Green's functions for different symmetries are already available in the literature.

Finally, by using the CGF, we can incorporate the effect of a free surface in the solid on the displacement and the strain fields caused by the nanoisland in the core as has been shown in [Tewary (2004)]. It is important to include the effect of at least one free surface because the strains are usually measured at or near a free surface. To account for a free surface, we use the Mindlin GF for  $\mathbf{G}(\mathbf{l}, \mathbf{l}')$  in Eq. (17) as has been done for a vacancy in copper [Tewary (2004)]. This retains the fully discrete atomistic nature of the core at the nano and sub-nano scales and links it seamlessly to the measurable macroscopic parameters of the continuum model like strains.

### 3 Gold Nanoisland in fcc Copper

For the purpose of illustration, we apply the GFMD method given in the preceding section to a gold nanoisland in an anisotropic semi-infinite crystal of fcc copper. We calculate the equilibrium position of the atoms in-

side and around the island and the displacement field and strains at the free surface. We assume that the free surface is (0,0,1) with the Z-axis of the coordinates normal to the free surface. We neglect the effect of other free surfaces so our results are valid when the nanoisland is much closer to the (0,0,1) surface as compared to other surfaces.

We use the tight-binding potential for copper, which has been given in the excellent paper by Cleri and Rosato (1993). The CR (Cleri-Rosato) potential extends up to fifth neighbor. It is a many-body potential that depends upon the coordinates of all 79 atoms that are within fifth neighbor distance of an atom. The potential correctly reproduces many static and dynamic properties of the solid including the cohesive energy, phonon dispersion, and the elastic constants. The force constants and the lattice statics GF for a million-atom perfect Cu lattice using the CR potential is calculated by using the techniques given in Tewary (1973), Maradudin et. al. (1971). The Mindlin GF for the anisotropic semi-infinite Cu with a free (0,0,1) surface is also given in Tewary (2004). The parameters of the CR potential for Cu-Cu, and Au-Cu are given by Cleri and Rosato (1993).

We create a nanoisland by replacing 63 Cu atoms by Au atoms while keeping the full point group symmetry of the fcc lattice. Thus  $n_A=63$ . The atom at the center of the nanoisland is assumed to be at the origin. All the lengths are in units of  $a$ , where  $2a=3.61 \text{ \AA}$  is the lattice constant of copper. The edge length of the inner core cube is  $2A=4$  which contains only Au atoms and gives a measure of the size of the Au nanoisland. The edge length of the outer core cube is  $2B=24$  and the shell cube  $2C=32$ . All the lattice sites in the shell and the outer core regions are occupied by Cu atoms. The size of the outer core is chosen so that it includes all the atoms that interact directly with the atoms in the inner core and the shell atoms do not interact directly with the atoms in the inner core. Similarly the size of the shell cube is chosen so that the host atoms outside the shell cube do not interact directly between the atoms in the outer core. The number of atoms in the outer core region is  $n_B=7750$  and in the shell region is  $n_C=10156$ . The total number of lattice sites in the super cell is  $10^6$ .

The equilibrium positions of the Au atoms inside the nanoisland and the Cu atoms around the Au nanoisland on the (0,0,1) plane are shown in Fig. 1 and on the (1,1,1) plane in Fig. 2. The empty circles denote the original lat-

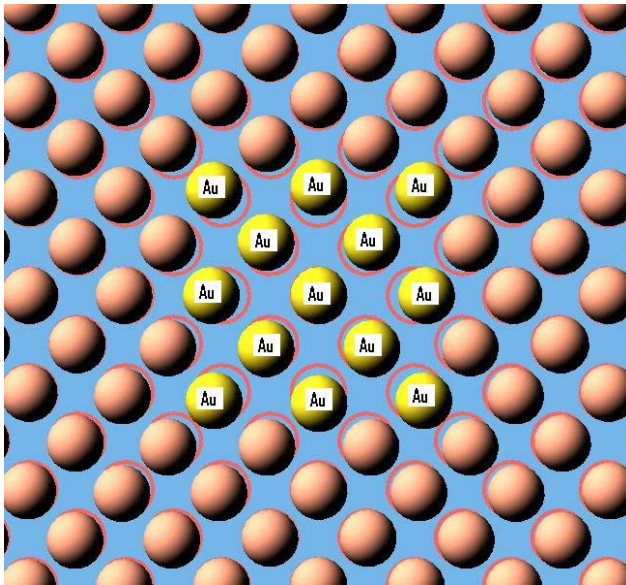


**Figure 1 :** Equilibrium position of the atoms in and around Au nanoisland in fcc Cu on the (0,0,1) plane. The empty circles denote the original lattice sites. Size of the circles is chosen arbitrarily for visualization. Au atoms as marked, Cu atoms unmarked.

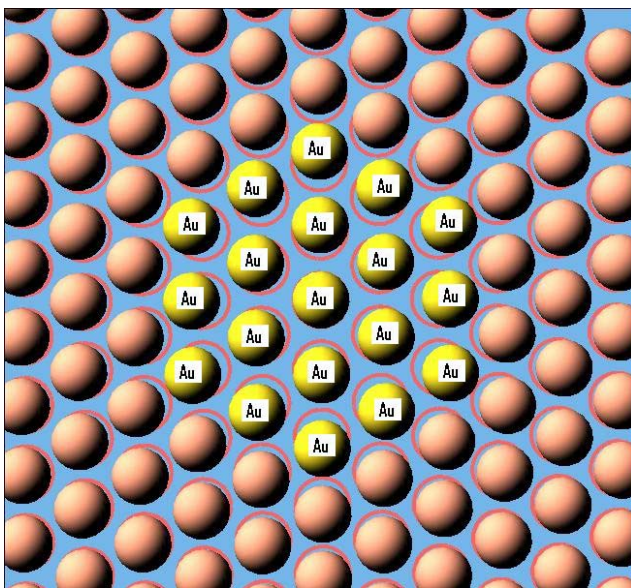


**Figure 2 :** Same as Fig. 1 on the (1,1,1) plane.

tice site in the reference lattice. The size of the circles has been chosen only for ease of visualization and bears no relation to the size of the atoms. We see from these fig-

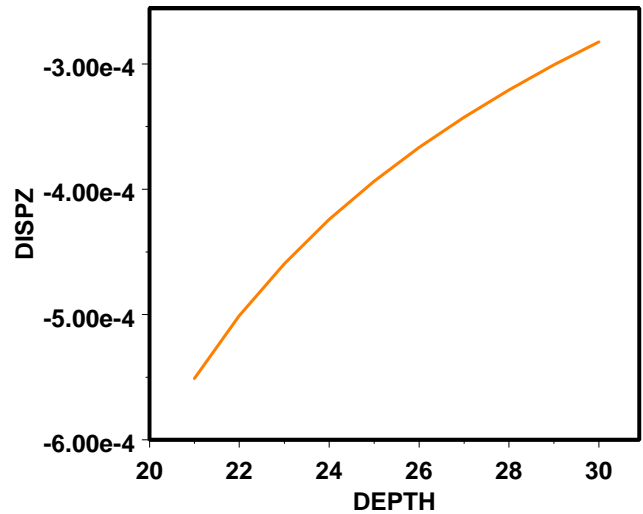
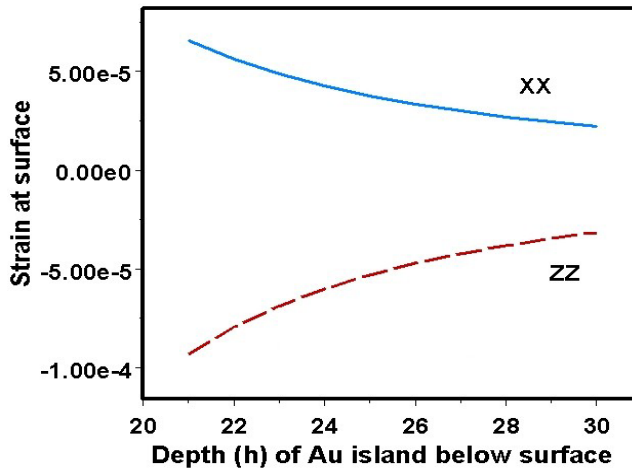


**Figure 3 :** Variation of  $u_z$ , the z-component of the displacement field on the (0,0,1) surface just above the Au nanoisland as a function of  $d$ , the distance of the central atom of the nanoisland from the free surface. All lengths in units of  $a=1.805 \text{ \AA}$ , half the lattice constant of fcc copper.

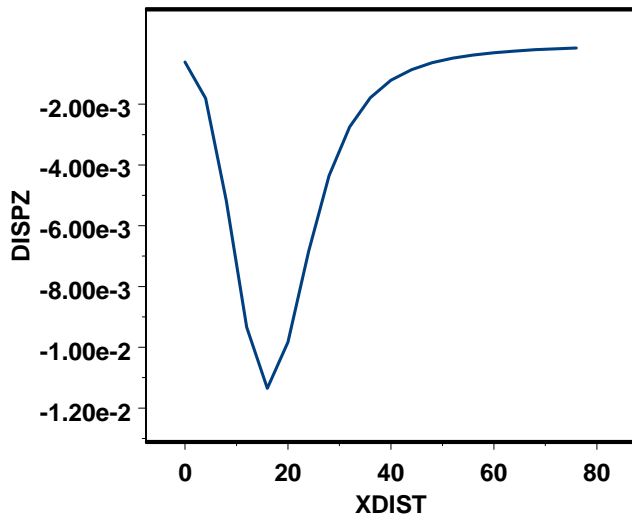
ures that, as expected, the atomic displacements are large inside and close to the core and decrease away from the core.

Figure 3 shows  $u_z$ , the z-component of the displacement field, on the free surface just above the Au nanoisland as a function of  $d$ , the depth of the nanoisland. The depth of the nanoisland is defined as the distance of the center of the nanoisland from the free surface. Figure 4 shows the strain components  $xx$  and  $zz$  for the same configuration. By symmetry,  $xx$  and  $yy$  components of the strain tensor are equal. The results are as expected that the displacement field as well the strain components at the surface decrease as the depth of the nanoisland decreases. The strain is about  $10^{-3}$ , which can be measured using modern techniques and can be used to characterize the nanoisland.

Figure 5 shows the variation of  $u_z$  and Fig. 6 shows the variation of the diagonal components of the strain tensor along the X-axis on the free surface for  $d = 21$ . Finally, Fig. (7) shows the 3D variation of  $u_z$  at the free surface for  $d=21$ . These figures show an interesting fact that the extrema at the surface of the displacement field as well the strains are not just above the center of the nanoisland



**Figure 4 :** The  $\epsilon_{xx} = \epsilon_{yy}$  and the  $\epsilon_{zz}$ -component of the strain tensor  $e$  on the  $(0,0,1)$  surface just above the Au nanoisland as a function of  $d$ .



**Figure 5 :** Variation of  $u_z$  on the X-axis on the  $(0,0,1)$  surface due to the Au nanoisland at  $d = 21$ .

but are slightly displaced. This behavior is a consequence of the elastic anisotropy and has also been found in a purely continuum calculation Yang and Tewary (2003) of InAs quantum dots in GaAs. Its consequences on the self assembly of nanostructures have been discussed by Yang and Tewary (2003).

The minimum value of  $d$  that we have assumed in our calculations is 21. The use of the continuum Green's function in our model as such is not valid when  $d$  is

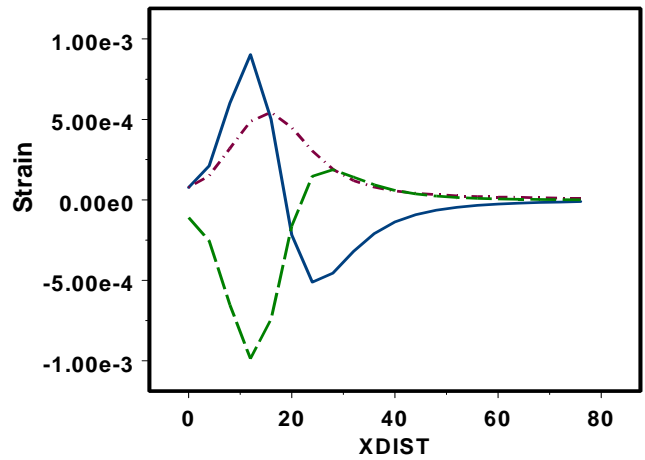


**Figure 6 :** Variation of  $\epsilon_{zz}$  (solid line),  $\epsilon_{xx}$  (long dashes), and  $\epsilon_{yy}$  (short dashes)

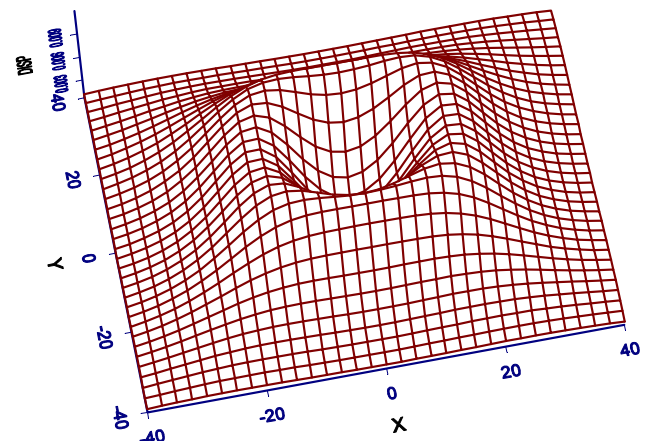


**Figure 7 :** Variation of  $u_z$  at the  $(0,0,1)$  surface due to the Au nanoisland at  $d = 21$ .

so small that the surface atoms are within the range of the interaction potential of the atoms in the shell region. At such small distances, the continuum parameters lose their significance anyway and one has to account for effects such as reconstruction of the surface, which is outside the scope of this work.

#### 4 Conclusions

We have described our GFMD technique for modeling a nanostructure in a semi-infinite solid containing a free surface. The technique combines the advantages of MD, lattice GF, and the continuum GF and thus links the

length scales from sub nano to macro. By linking MD with the LSGF, we can include the nonlinear effects in the core of the defect, and by using the LSGF model a large crystallite (million-atoms or more) without excessive CPU requirements. For example, calculation of the LSGF for a million atom crystallite requires only a few seconds on a standard 3 GHz desktop.

By using the asymptotic relationship between the LSGF and the CGF, we can incorporate the effect of extended defects such as a free surface, interfaces in the host lattice, dislocations, etc. This relationship also enables us to relate discrete atomic displacements with measurable macroscopic elastic parameters such as strains or displacement field at the free surface without any need for an arbitrary averaging ansatz.

In the GFMD model we express the response of the solid in terms of effective Kanzaki forces and the perfect LSGF which is exactly equivalent to using the Dyson's equation for calculating the defect GF. By including the nonlinear effects fully and exactly in the forces, our model is able to relate the physical processes in the core to the response of the lattice at the macro scales in the entire solid. Since the LSGF can be calculated for a large crystallite without excessive CPU requirements, our calculated values of the atomic displacements in the bulk of the solid would not suffer from spurious size effects which can often affect the conventional MD calculations.

We have applied the GFMD method to calculate the atomistic configuration of a Au nanoisland in fcc copper containing a free (0,0,1) surface. The resulting displacement and the strain fields are calculated at the free surface, which are measurable parameters at the macroscopic scale. This shows the multiscale nature of our model that seamlessly links the interatomic length scales in the core of the nanoisland to measurable macroscopic scales.

**Acknowledgement:** This work was supported in part by the NIST Advanced Technology Program. The authors thank Dr. C. Flannery and Dr. T.P. Quinn for their helpful comments on the manuscript.

## References

- Binns, C.** (2001): Nanoclusters deposited on surfaces. *Surface Science Reports*, vol. 44 (1-2), pp. 1-49.
- Cleri, F.; Rosato, V.** (1993): Tight-binding potentials for transition-metals and alloys. *Phys. Rev.*, vol. B 48, pp. 22-33.
- Ghoniem, N. M.; Cho, K.** (2002): The Emerging Role of Multiscale Modeling in Nano- and Micro-mechanics of Materials, *CMES: Computer Modeling in Engineering & Sciences*, vol. 3, pp. 147-174.
- Maradudin, A. A.; Montroll, E. W.; Weiss, G. H.; Ipatova, I. P.** (1971): *Theory of lattice dynamics in the harmonic approximation*, *Solid State Physics*, Academic Press, NY. Second edition. Editors: Ehrenreich, H.; Seitz, F.; Turnbull, D.: supp 3.
- Ortiz, M.; Phillips, R.** (1999): Nanomechanics of defects in solids. *Adv. Applied Mech.*, vol. 36, pp. 1-79.
- Palacios, F. J.; Iniguez, M. P.; Lopez, M. J.; Alonso, J. A.** (1999): Molecular-dynamics study of the structural rearrangements of Cu and Au clusters softly deposited on a Cu (001) surface. *Phys. Rev.*, B vol. 60, pp. 2908-2915.
- Pan, E.; Yang, B.** (2001): Elastostatic fields in an anisotropic substrate due to a buried quantum dot. *J. Appl. Phys.*, vol. 90, pp. 6190-6196.
- Pan, E.** (2002): Mindlin's problem for an anisotropic piezoelectric half-space with general boundary conditions. *Proc. Royal Soc. (Lond)*, vol. 458, pp. 181-208.
- Pan, E.; Yuan, F. G.** (2000): Three-dimensional Green's functions in anisotropic bimetals. *Int. J. Solids Struct.*, vol. 37, pp 5329-5351.
- Phillips, R.** (1998): Multiscale modeling in the mechanics of materials. *Current Opinion in Solid State Materials Science*, vol. M 3, pp 526-532.
- Rao, S.; Hernandez, C.; Simmons, J. P.; Parthasarathy, T. A.; Woodward, C.** (1998): Green's function boundary conditions in two-dimensional and three-dimensional atomistic simulations of dislocations. *Phil. Mag.*, vol. 77, pp 231-256.
- Sandberg, N.; Grimvall, G.** (2001): Anharmonic contribution to the vacancy formation in Cu. *Phys. Rev.*, vol. B 63, article number 184109.
- Shen, S.; Atluri, S. N.** (2004): Multiscale Simulation Based on the Meshless Local Petrov-Galerkin (MLPG) Method, *CMES: Computer Modeling in Engineering & Sciences*, vol. 5, pp. 235-256.
- Srivastava, D.; Atluri, S. N.** (2002): Computational Nanotechnology: A Current Perspective, *CMES: Computer Modeling in Engineering & Sciences*, vol. 3, pp. 531-538.

**Sinclair, J. E.; Gehlen, P. C.; Hoagland, R. G.; Hirth, J. P.** (1978): Flexible boundary conditions and non-linear geometric effects in atomic dislocation modeling. *J. App. Phys.*, vol. 49, pp 3890-3897.

**Tadmor, E. B.; Ortiz, M.; Phillips, R.** (1996): Quasi-continuum analysis of defects in solids. *Phil. Mag.*, vol. A73, pp 1529-1563.

**Tewary, V. K.** (2002): Change in low-temperature thermodynamic functions of a semiconductor due to a quantum dot. *Phys. Rev.*, vol. B66, article number 205321.

**Tewary, V. K.** (2004): Multiscale Green's-function method for modeling point defects and extended defects in anisotropic solids: application to a vacancy and free surface in copper. *Phys. Rev.*, vol. B69, article number 094109.

**Tewary, V. K.** (1973): Green's function method for lattice statics. *Advances in Physics*, vol. 22, pp 757-810.

**Tewary, V. K.; Yang, B.** (2003): Multiscale modeling of mechanical response of quantum nanostructures. In Bahr, D.F.; Kung, H.; Moody, N.R.; Wahl, K.J (editors) *Mechanical Properties Derived from Nanostructuring Materials*, Symposium Proceedings vol. 778, Materials Research Society, Warrendale, PA. pp. 297-302.

**Thomson, R.; Zhou, S.; Carlsson, A. E.; Tewary, V. K.** (1992): Lattice imperfections studied by use of lattice green-functions. *Phys. Rev.*, vol. B46, pp 10613-10622.

**Ting, T. C. T.** (1996): *Anisotropic Elasticity*, Oxford University Press, Oxford.

**Vashishta, P.; Kalia, R. K.; Nakano, A.** (2003): Multi-million atom molecular dynamics simulations of nanostructures on parallel computers. *J. Nanoparticle Research*, vol. 5, pp. 119-135.

**Yang, B.; Tewary, V. K.** (2003): Formation of a surface quantum dot near laterally and vertically neighboring dots. *Phys. Rev.*, vol. B 68, article number 035301.

**Zhigilei, L. V.; Dongare, A. M.** (2002): Multiscale Modeling of Laser Ablation: Applications to Nanotechnology, *CMES: Computer Modeling in Engineering & Sciences*, vol. 3, pp. 539-556.

